

Review

ImmunoPET Directed to the Brain: A New Tool for Preclinical and Clinical Neuroscience

Ángel García de Lucas^{1,2,3,*} , Urpo Lamminmäki³  and Francisco R. López-Picón^{1,2} ¹ PET Preclinical Imaging Laboratory, Turku PET Centre, University of Turku, 20520 Turku, Finland² MediCity Research Laboratory, University of Turku, 20520 Turku, Finland³ Department of Life Technologies, University of Turku, 20520 Turku, Finland

* Correspondence: angel.garciadelucas@utu.fi

Abstract: Immuno-positron emission tomography (immunoPET) is a non-invasive in vivo imaging method based on tracking and quantifying radiolabeled monoclonal antibodies (mAbs) and other related molecules, such as antibody fragments, nanobodies, or affibodies. However, the success of immunoPET in neuroimaging is limited because intact antibodies cannot penetrate the blood–brain barrier (BBB). In neuro-oncology, immunoPET has been successfully applied to brain tumors because of the compromised BBB. Different strategies, such as changes in antibody properties, use of physiological mechanisms in the BBB, or induced changes to BBB permeability, have been developed to deliver antibodies to the brain. These approaches have recently started to be applied in preclinical central nervous system PET studies. Therefore, immunoPET could be a new approach for developing more specific PET probes directed to different brain targets.

Keywords: positron emission tomography; neuroimaging; immunoPET; brain; blood–brain barrier; antibody engineering; neuroscience; neuro-oncology; neurology; neuropsychiatry

**Citation:** de Lucas, Á.G.;

Lamminmäki, U.; López-Picón, F.R.

ImmunoPET Directed to the Brain: A New Tool for Preclinical and Clinical Neuroscience. *Biomolecules* **2023**, *13*, 164. <https://doi.org/10.3390/biom13010164>

Academic Editor: Hervé Boutin

Received: 21 December 2022

Revised: 8 January 2023

Accepted: 10 January 2023

Published: 13 January 2023



Copyright: © 2023 by the authors. Licensee MDPI, Basel, Switzerland. This article is an open access article distributed under the terms and conditions of the Creative Commons Attribution (CC BY) license (<https://creativecommons.org/licenses/by/4.0/>).

1. Introduction

Immuno-positron emission tomography (immunoPET) is a non-invasive in vivo imaging method based on tracking and quantifying radiolabeled monoclonal antibodies (mAbs) and other related molecules, such as antibody fragments, nanobodies, or affibodies [1,2]. Antibody imaging provides a specific and sensitive means of non-invasively characterizing the cell surface phenotype in vivo, which aids in diagnosis, prognosis, therapy selection, and monitoring of treatment for many diseases [3]. Since its inception, the field of immunoPET has been focused on oncology research because mAbs play an important role in the clinical management of cancer [4,5]. In addition to cancer, this technology is attractive for improving our knowledge in the diagnosis of brain disorders, as it is difficult to obtain biosamples from the brain [6]. However, the success of immunoPET in neuroimaging is limited because intact antibodies poorly penetrate the blood–brain barrier (BBB). Due to the poor permeability of the BBB, the delivery of therapeutic bioactive macromolecular compounds to the central nervous system (CNS) is difficult to achieve [7]. For example, only 0.1% of peripherally administered antibodies are delivered into the mouse brain [8]. To overcome this problem, different non-invasive methods have been developed to enhance antibody delivery to the CNS.

PET imaging studies of the CNS initially focused on global or regional changes in brain function, such as glucose utilization, cerebral blood flow, and oxygen metabolism. However, according to our knowledge of the diversity of neurotransmitter systems has been growing, we need to develop molecular imaging probes with an even higher target specificity than first-generation PET radiotracers [9]. Similar to CNS drug discovery, PET radiotracer development for the brain is scientifically challenging, with success being quite sporadic. Primarily, the radiotracer must show high affinity and selectivity for the target protein. Moreover, the radiotracer must be able to reach its target in vivo [10].

Therefore, the immunoPET approach could accelerate PET research in the brain to increase the development of new and more specific imaging probes.

The purpose of this literature review is to outline the major contributions of immunoPET to preclinical and clinical neurosciences. First, we write about strategies to cross the BBB, antibody design, and radiolabel. After that, we summarize the principal advances in neuro-oncology and neurological diseases. Finally, we hypothesize the development of immunoPET in these areas and the future possibilities for neuropsychiatry. Other extensive recent reviews can be found in the diagnosis of glioblastoma diagnosis [11] and Alzheimer's disease research [6].

2. Strategies to Cross the BBB

Different strategies have been used to deliver antibodies into the brain, including modifications in their physicochemical properties; physiological mechanisms, such as adsorption-mediated transcytosis (AMT) or receptor-mediated transcytosis (RMT); and induced changes in BBB permeability (Table 1).

Table 1. Summary of different strategies to cross the BBB with proteins or antibodies.

Strategy	Mechanism	References
Physicochemical properties modification	Poly(ethylene glycol) conjugation to increase the circulation half-life	[12,13]
Through physiological mechanism	Cationic proteins or nanobodies that trigger adsorption-mediated transcytosis (AMT)	[14–16]
	Ligands or antibodies that trigger receptor-mediated transcytosis (RMT)	[17–32]
BBB permeability changes	Open BBB with solvents such as mannitol	[19,33]
	Focused ultrasound (FUS) with microbubbles	[34–38]

One physicochemical modification strategy is to increase the circulation half-life of antibodies, such as coupling poly(ethylene glycol) (PEG) to antibodies [12]. Prolonged circulation results in greater serum concentrations, which drive a greater accumulation of antibodies in low-permeability organs, such as the brain. In addition, PEG can act as a ligand for cholesterol transport receptors to promote the active transport of macromolecules into the brain [13].

Various cationic proteins can cross the BBB through AMT [14]. Upon electrostatic interactions between the cationized protein and anionic charges present on the surface of epithelial cells of BBB, the endocytosis of cationized proteins is triggered, a preliminary step for the protein to cross the BBB [15]. The variable heavy-chain domain of camel homodimeric antibodies (VHH) or nanobodies with a high isoelectric point (pI) have demonstrated an ability to cross the BBB through this mechanism [15,16].

RMT begins with the binding of a ligand to its cognate receptor on the luminal membrane of the brain's microvascular and capillary endothelial cells. It is a multistage process involving receptor-mediated endocytosis, mediated by clathrin-coated or non-clathrin-coated vesicles, followed by intracellular trafficking and vesicular sorting, finally resulting in vesicle fusion with the abluminal membrane of the BBB and delivery of the contents to the brain parenchyma [17]. Several receptors capable of inducing RMT are present in the BBB, such as the insulin receptor, transferrin receptor (TfR), and receptors responsible for lipoprotein transport, whereas others, such as the albumin receptor, are not expressed [18]. Antibodies can be modified to pass into the brain by conjugation with specific BBB receptor ligands [19]. For instance, antibodies targeting the transferrin receptor have been reported to cross the BBB [20]. Bivalent binding to TfR induces lysosomal sorting and degradation consistent with the incomplete transcellular trafficking observed *in vivo*, but monovalent binding leads to successful transcytosis in the BBB [21]. This brain shuttle strategy has been used successfully for immunoPET in animal models of Alzheimer's, which are reviewed below [22–32].

The first attempt to modify the permeability of the BBB was in 1981 using mannitol, which was administered together with a drug, methotrexate, to enhance its delivery to brain tumors [33]. In the same way, other solvents, such as ethanol, dimethylsulfide, etoposide, or histamine, have been used to open the BBB and facilitate the delivery of drugs to the brain. However, the opening of the BBB is nonselective; thus, the use of these agents to affect the permeability of the BBB can cause serious side effects [19]. A more non-invasive, local, and targeted way to disrupt the BBB is with focused ultrasound (FUS). This technique, in combination with microbubbles, can lead to the transient and focal opening of the BBB, enabling the passage of therapeutic agents across the BBB without relying on the enhanced permeability and retention effect (EPR) [34]. Antibodies have successfully been delivered into the brain using FUS [35–38]. In addition, two studies have used an immunoPET approach to detect radiolabeled antibodies in gliomas [37,38].

3. Antibody Engineering Strategies for ImmunoPET

Antibodies' capacity to cross the BBB, which is inherently limited for native antibodies [39], can be significantly improved by endowing the antibody with the capability to use RMT. This is achieved by generating bispecific antibodies that can bind both the RMT-associated receptor, such as TfR or insulin receptor and the target of interest in the CNS. The modular structure of the antibody molecule makes it possible to create bispecific antibodies of many different designs [40], including asymmetric IgG-like constructs in which the binding specificity of one of the two inherently identical binding sites has been altered [41–43]. In another common type of construct, antibody fragment(s) providing the second binding specificity are genetically fused to IgG [24,44,45]. Typically, single chain Fv (scFv) fragments consisting of the light and heavy chain variable domains linked together with a peptide linker of approximately 15–20 amino acids are used in such constructs. Yet another way to generate bispecific constructs is to conjugate two or more antibody fragments with different binding specificities together with peptide linkers [29,46,47]. Figure 1 shows an example of each of these three types of the bispecific antibody. Recently, Kariolis et al. reported a strategy to endow IgG with a capacity to bind TfR for RMT without modifying or adding variable domains for the second binding specificity. Instead, they engineered the surface of the C-terminal domain of the Fc-part to introduce a binding site for TfR [48]. In addition to the use of genetic engineering, chemical conjugation has also been employed for generating bispecific binders [22].

In addition to IgGs or fragments of them, other types of bioaffinity proteins can be utilized for the generation of bispecific targeting proteins, including single immunoglobulin domain-based binders obtained from camelid animals [49] or sharks [31] and alternative protein scaffolds, such as affibodies [2] and DARPins [50]. For bispecific binding, two or more such binders can be linked together with peptide linkers, or these binders can be linked to IgG instead of scFvs. In addition to being smaller (5–20 kDa) than scFvs, the alternative scaffold-based binders present various other benefits over antibody fragments, including higher stability and good expression properties. Overall, the ability to use a variety of antibody formats, alternative binders, and their potential combinations opens up a plethora of options for developing bispecific bioaffinity molecules with different types of structural and functional characteristics [51].

The bispecific designs can be assigned to two categories based on the presence or absence of the Fc-part of immunoglobulin. The presence of the Fc-part increases the circulation half-life of the antibody construct considerably due to FcRn-mediated rescue from lysosomal degradation. The Fc also contributes to the size of the construct by approximately 50 kDa. Overall, the Fc-part, whether present or absent, has a significant effect on the distribution and clearance of antibody constructs in the body [52] and affects the performance of antibody-based imaging agents.

Another important feature to consider in the bispecific designs is the binding valency (e.g., the number of binding sites for a specific antigen in the construct). Typically, there is either one or two binding sites of each specificity in a bispecific construct. Due to the

bivalency of native IgG, the use of an asymmetric design is typically required to obtain monovalent binding with an IgG-based construct (Figure 1A). Compared to monovalent binding, bivalent binding can significantly increase the strength of the interaction with multimeric targets [53]. On the other hand, even in the presence of more than one binding site of certain specificity, the dimensions and flexibility of the constructs can affect the availability of the binding sites within it and, thus, the antibody's mode of binding. For example, a construct with two TfR binding scFvs linked to the C-terminus of the light chains of IgG with short peptide linkers exhibits monovalent interaction with the dimeric TfR, suggesting that the limited flexibility of the construct hinders the simultaneous binding of the two scFvs [24].

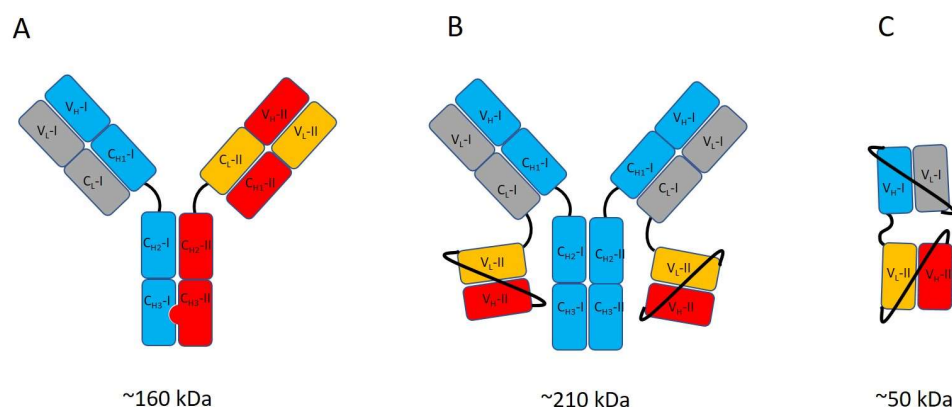


Figure 1. Examples of bispecific antibody constructs. (A) IgG-like asymmetric antibody engineered to bind an RMT-associated target with one of its binding arms and the CNS-associated target with the other binding arm. The knob-into-hole approach [41] is used to guide correct pairing of two different heavy chains, and CrossMab technology [42] is used to prevent mispairing of the light chains. (B) IgG-like antibody with scFv fragments of different binding specificity conjugated to the C-terminus of the light chains. This is a symmetric IgG-based construct. (C) di-scFv construct in which two scFvs with different binding specificities are fused together via a short peptide linker. V_L and V_C refer to the light chain variable and constant domains, respectively. V_H , C_{H1} , C_{H2} and C_{H3} refer to the heavy chain variable domain and the constant domains 1, 2 and 3, respectively. The roman numbers in the domain names (e.g., V_L -I or V_L -II) show which of the two different binding specificities the domain is associated to.

Complex artificial antibody designs, typical in bispecific antibodies, tend to have an elevated risk of liabilities related to their biochemical or biophysical properties, including limited stability, low expression yields, a tendency to aggregate or poor pharmacokinetics [51,54]. These issues can sometimes be tackled or alleviated by further optimizing the antibody via genetic engineering, but the process can be time-consuming.

Genetic engineering can also be used to modify the binding sites of the antibody to optimize the strength of the binding. The two different binding sites of a bispecific antibody can differ in terms of the optimal binding affinity. When it comes to binding the actual imaging target, high-affinity binding is generally considered to be beneficial for successful immunopET imaging. The situation can be different with the recognition of the RMT target; too high an affinity towards TfR can make the antibody stick to the receptor too tightly [20], increasing the likelihood of its lysosomal degradation instead of RMT. On the other hand, a too-weak affinity can impede the accumulation of antibodies in the cells of the BBB.

4. Radiolabeling Strategies

PET scans detect positron-emitting radionuclides, which are attached to a molecule such as a protein or an antibody. The positron is created, being short-lived, and eventually gets annihilated, converting all its mass into energy and thereby emitting two photons of

511 keV each (which is the resting energy of the electron or positron) in opposite directions. These two photons are detected in coincidence by scintillation detectors of PET scan [55].

Key to the labeling of antibodies, and antibodies-related molecules, is the appropriate matching between the biological half-life of the protein and the physical half-life of the radionuclide [2,56]. The shorter-lived PET radionuclides ^{11}C , ^{18}F , ^{68}Ga , ^{44}Sc , and ^{64}Cu have been used for radiolabeling antibody fragments, while the slow pharmacokinetics of intact antibodies have enabled the use of the long-lived nuclides ^{89}Zr and ^{124}I [2]. PET radionuclides characteristics used to label antibodies and antibody fragments are summarized in Table 2.

Table 2. Summary of PET radionuclides characteristics used in immunoPET. Data extracted from [57,58].

Radionuclide	Half-Life	Branching Ratio (B^+) (%)	Positron Energy– E_{Max} [Mev]	Mean Positron Range (mm)
^{11}C	20.4 min	99	0.97	1.2
^{18}F	109.7 min	97	0.65	0.6
^{68}Ga	67.7 min	89	1.90	3.5
^{44}Sc	3.97 h	94	1.47	2.3
^{64}Cu	12.7 h	18	0.65	0.7
^{89}Zr	78.4 h	23	0.91	1.3
^{124}I	100.2 h	23	1.54	4.4

The labeling of proteins can be performed by direct labeling, the addition of a prosthetic group, or using bifunctional chelators. Direct labeling, which nowadays involves mostly radioiodination, is the method used to label proteins without using intermediates such as prosthetic groups or bifunctional chelators. Prosthetic groups are small molecules able to bind with radionuclides in one site of the structure and simultaneously with a protein at a second site. An example of this procedure is the modification of the protein to bear unnatural biorthogonal functional groups such as an azide and then by using “click” chemistry to achieve the radiolabeled biomolecule. Radiometals (^{68}Ga , ^{44}Sc , ^{64}Cu , and ^{89}Zr) require bifunctional chelators, which are capable of coordinating a metal ion, and can be attached to the proteins. There are two main types of bifunctional chelators: cyclic, such as 1,4,7,10-tetraazacyclododecane-1,4,7,10-tetraacetic acid (DOTA) and 1,4,7-triazacyclononane-1,4,7-triacetic acid (NOTA); and acyclic multidentate, such as desferrioxamine B (DFO) and diamine-pentaacetic acid (DTPA) [59]. DOTA and NOTA chelation methods have been the mainstay for ^{64}Cu labeling of antibody fragments. The DFO ligand is commonly used to chelate ^{89}Zr due to its high chelation yields, mild reaction conditions, and reasonable stabilities [2]. In addition, several studies have shown that DFO, as well as NOTA, are suitable chelators for radiolabeling of biomolecules with ^{68}Ga [2,60]. Finally, CHX-A''-DTPA (*N*-[(*R*)-2-amino-3-(para-isothiocyanato-phenyl) propyl]-trans-(*S,S*)-cyclohexane-1,2-diamine-*N,N,N',N'',N''*-pentaacetic acid) has been identified as the most promising choice for ^{44}Sc , as it permits labeling at room temperature within a reasonable period of time [61].

The long-lived radionuclides, such as ^{89}Zr and ^{124}I , are compatible with the long circulation of antibodies or antibody fragments, but they can result in high radiation burden and low image quality due to the long positron range [62]. To try to overcome this, a pre-targeting approach allows combining long circulating antibodies or antibody fragments with short-lived PET radionuclides such as ^{18}F or ^{11}C . In the pre-targeting approach, an antibody is chemically tagged, injected, and allowed enough time to accumulate in the target regions, and washout from non-target tissues and blood. Afterward, a radiolabeled small molecule that can rapidly react with the tag in the antibody is injected [63–65]. The combined use of the “click” reacting trans-cyclooctene (TCO) derivatives as chemical tags,

and tetrazine (Tz) derivatives as radiolabeled small molecules, are the state of the art for pre-targeted PET imaging [66].

Recently developed bi-specific antibodies that penetrate the BBB by targeting transferrin [22–32] could be labeled with TCO for a pre-targeting approach across the BBB. The various ^{18}F -labeled Tzs used for pre-targeting approaches in rodent cancer models and that could be used for neuroimaging studies, unfortunately, do not cross the BBB due to unfavorable characteristics [67]. Very recently, Shalgunov et al. developed a series of ^{18}F -labelled Tzs that successfully penetrated the BBB in rodents and clicked *in vivo* with a TCO-polymer injected into the brain. The lead compound in this study is a promising tool for future pre-targeted neuroimaging studies [68].

5. Current Applications

5.1. Neuro-Oncology

In 2010, brain metastases were first visualized in HER2-positive breast cancer patients using [^{89}Zr]Zr-DFO-trastuzumab. This study demonstrated brain lesions with an 18-fold higher [^{89}Zr]Zr-DFO-trastuzumab uptake in tumors than in normal brain tissue. The brain penetration of [^{89}Zr]Zr-DFO-trastuzumab was possible because of a disruption of the BBB at the site of the brain metastasis [69]. Another study in HER2-positive breast cancer patients using [^{89}Zr]Zr-DFO-pertuzumab demonstrated the detection of brain metastases in these patients [70]. In HER2-negative metastatic breast cancer patients, immunoPET following a pre-targeting approach against carcinoembryonic antigen (CEA) showed higher overall sensitivity than [^{18}F]FDG PET imaging in disclosing metastases, including brain dissemination [71]. In rodents, HER2-positive intracranial breast carcinoma xenografts have been shown to uptake of an ^{18}F -labeled single-domain antibody fragment [72].

In addition to brain metastasis, most high-grade gliomas lead to the destruction of the BBB, with subsequent leakage of contrast medium, which is not shown by low-grade gliomas [73]. This increased permeabilization in high-grade gliomas, such as glioblastoma multiforme (GBM), could be used to deliver antibody-based therapeutics or immunoPET probes. In this sense, several preclinical studies have been conducted with different targets: integrin $\alpha\text{v}\beta 3$ [74], epidermal growth factor receptor (EGFR) [61,75,76], delta-like ligand 4 (Dll4) [77], cluster of differentiation 105 (CD105) [75], fibroblast activation protein alpha (FAP) [78], CD146 [79,80], membrane-type 1 matrix metalloproteinase (MT1-MMP) [81], CD11b [82], vascular endothelial growth factor (VEGF) [83–85], transforming growth factor- β (TGF- β) [86,87], and prostate-specific membrane antigen (PSMA) [88,89]. In the early stages of this field, some studies with different immunoPET approaches were conducted in GBM flank xenograft models [61,74,75,77–79]. In addition to these models, orthotopic xenograft mice models were used to demonstrate the capacity of [^{64}Cu]Cu-NOTA-YY146 to penetrate the disrupted BBB and efficaciously target CD146 within brain tumors, demonstrating that expression levels of CD146 can be scrutinized non-invasively in high-grade gliomas with PET imaging for potential patient selection and stratification for targeted therapies [80]. Another study that used orthotopic GBM xenograft models demonstrated the feasibility of using an immunoPET probe ([^{89}Zr]Zr-DFO-LEM2/15) on MT1-MMP marker to visualize GBM tumors for diagnostic purposes. [^{89}Zr]Zr-DFO-LEM2/15 was able to detect orthotopically growing GBM implants from TS543 (Figure 2A) but not U251, which correlates with the integrity of the BBB, as analyzed by Evans blue staining [81]. Therefore, the integrity of the BBB is one of the major limitations for the use of antibodies in high-grade gliomas because all GBM have clinically significant regions of tumor with an intact BBB [90]. In addition to targeting tumor cells, tumor-associated myeloid cells (TAMCs) can be an interesting immunoPET target because, in GBM, the immunosuppression is largely mediated by these cells. The [^{89}Zr]Zr-DFO-anti-CD11b antibody PET imaging probe enabled the surveillance of immunosuppressive TAMCs in the tumor microenvironment of a mouse orthotopic glioma model, thereby providing a means of assessing the efficacy of immunotherapy [82].

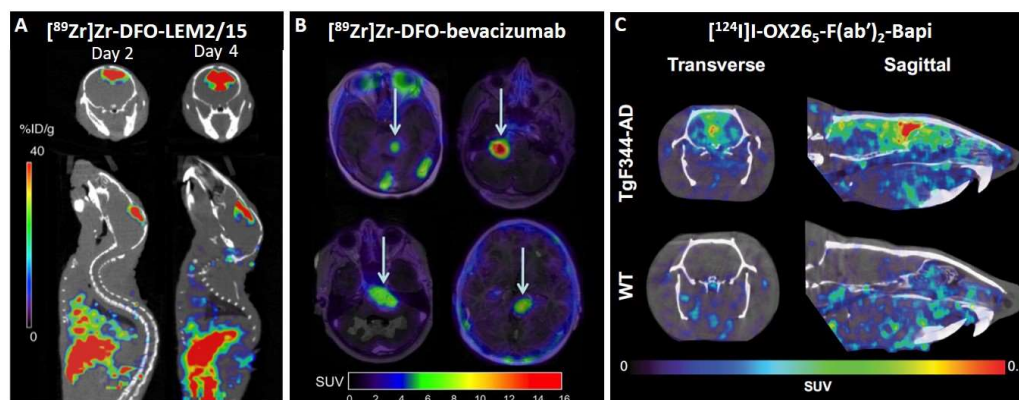


Figure 2. Examples of immunoPET images in preclinical and clinical neuroscience. (A) Representative fused PET/CT images of coronal and sagittal planes at 2 and 4 days post-injection containing TS543 brain tumors with $[^{89}\text{Zr}]\text{Zr-DFO-LEM2/15}$. (Image: Adapted from Ref. [81]). (B) PET/MR fusion images of four different pediatric patients with DIPG where four tumors showed variable uptake of $[^{89}\text{Zr}]\text{Zr-DFO-bevacizumab}$ (arrows). (Image: Adapted from Ref. [84]). (C) Representative in vivo PET images from TgF344-AD and WT rats 3 days post-administration of $[^{124}\text{I}]\text{I-OX265-F(ab')}_2\text{-Bapi}$. (Image: Adapted from Ref. [32]).

One interesting example of fast translation from the preclinical to the clinical field is $[^{89}\text{Zr}]\text{Zr-DFO-bevacizumab}$ PET imaging in diffuse intrinsic pontine glioma (DIPG) [83–85]. Bevacizumab is a recombinant humanized monoclonal antibody against VEGF that has demonstrated significant responses and prolonged survival in individual patients with DIPG [91,92]. Therefore, the challenge is to identify patients who will benefit from treatment with bevacizumab [84]. In the first research paper, $[^{89}\text{Zr}]\text{Zr-DFO-bevacizumab}$ was used to study its biodistribution in different intracranial and subcutaneous murine tumor models, and accumulation of this antibody was only observed in the subcutaneous tumor models. These results are in line with the poor clinical response rates obtained with bevacizumab thus far in children with DIPG. Consequently, this research suggests that bevacizumab treatment is only justified if the tumor has been previously detected using $[^{89}\text{Zr}]\text{Zr-DFO-bevacizumab}$ [83]. One year later, a first pilot immunoPET study in pediatric DIPG patients suggested that the addition of $[^{89}\text{Zr}]\text{Zr-DFO-bevacizumab}$ PET imaging (Figure 2B) may help in selecting potential candidates for bevacizumab treatment of DIPG because this procedure assesses both target availability and drug accessibility of the tumor [84]. Subsequently, a study was performed with a 1-on-1 analysis of multiregional in vivo and ex vivo $[^{89}\text{Zr}]\text{Zr-DFO-bevacizumab}$ uptake, tumor histology, and vascular morphology in a DIPG patient. PET imaging was capable of detecting heterogeneity in $[^{89}\text{Zr}]\text{Zr-DFO-bevacizumab}$ uptake between lesions, which correlated well with the ex vivo measurements. However, PET cannot detect subcentimeter intralesional uptake heterogeneity [85]. Another clinical study demonstrated that a radiolabeled antibody against TGF- β , $[^{89}\text{Zr}]\text{Zr-DFO-fresolimumab}$, reaches recurrent high-grade gliomas. However, monotherapy with fresolimumab did not result in an antitumor effect [86]. Interestingly, a recent preclinical research paper in which $[^{89}\text{Zr}]\text{Zr-DFO-fresolimumab}$ was used to detect radiation-induced TGF- β activation in tumors suggested that fresolimumab could improve the outcome of radiotherapy [87]. Finally, anti-PSMA radiolabeled antibody, $[^{89}\text{Zr}]\text{Zr-DFO-huJ591}$, was studied in a 51-year-old woman diagnosed 8.5 years ago with grade II oligodendroglioma (1p/19q co-deleted, IDH mutant) and disease progression despite multiple prior treatments, including surgery and chemo-radiation, most recently with IDH inhibitor AG-120 (NCT02074839). $[^{89}\text{Zr}]\text{Zr-DFO-huJ591}$ uptake was observed in two brain lesions determined to be anaplastic oligodendroglioma (grade III) histologically [88]. In addition to intact antibodies in clinical research, a radiolabeled minibody against PSMA, $[^{89}\text{Zr}]\text{Zr-DFO-IAB2M}$, was tested in two high-grade gliomas and metastatic brain tumors from lung cancer patients. $[^{89}\text{Zr}]\text{Zr-DFO-IAB2M}$ may have potential value in the differen-

tial diagnosis of high-grade glioma from primary CNS lymphomas (PCNSL) or radiation necrosis, as well as in the prediction of treatment efficacy and assessment of the treatment response to bevacizumab therapy for high-grade glioma [89].

5.2. Neurological Diseases

The first attempts to reach the brain with a preclinical immunoPET approach used poly(ethylene glycol) antibodies against amyloid- β (A β). ^{64}Cu -labeled anti-A β mAbs 6E10, M116, and M31, showed differences in uptake between the TgCRND8 mouse model of Alzheimer's disease and wild-type animals [12,13]. In addition, radiolabeled antibodies without specific modification to cross the BBB were studied in Alzheimer's rodent models. However, limited penetration made them inadequate for monitoring cerebral amyloid pathogenesis [93,94].

The first successful bispecific antibody-based brain PET study was performed in 2016. A human version of mAb158 F(ab')₂ fragment against soluble A β protofibrils was chemically conjugated to 8D3 TfR antibody and radiolabeled with iodine-124. [^{124}I]I-8D3-F(ab')₂-h158 was taken up into the brain through TfR-mediated transcytosis, and A β was detected in the tg-ArcSwe and tg-Swe Alzheimer mouse models [22]. Age or genotype did not influence the systemic pharmacokinetics or biodistribution to major organs [23]. In these studies, PET imaging correlated with age and A β pathology in the brains of Alzheimer's mouse models [22,23]. However, the chemical conjugation resulted in a heterogeneous mixture of fusion proteins randomly linked together at different positions, which is not suitable for clinical application. In addition, the use of the complete 8D3 antibody resulted in bivalent TfR binding, which has been shown to be suboptimal for transcytosis. Therefore, a new format was created in which the C-terminal end of the RmAb158 light chain was attached to the scFv of 8D3. In this way, monovalent interactions were achieved with TfR despite having two binding sites, improving transfer across the BBB, with higher or equal brain uptake compared to previously reported BBB shuttles at both trace and therapeutic doses [24]. [^{124}I]I-RmAb158-scFv8D3 demonstrated an ability to follow disease progression and detect the effects of β -secretase inhibitor treatment by PET imaging in different mouse models of Alzheimer's disease and was able to detect quantitative differences between treated and untreated groups, whereas [^{11}C]Pittsburgh compound B ([^{11}C]PiB) PET did not detect any differences between treated and untreated groups [25,26]. RmAb158-scFv8D3 and 8D3-F(ab')₂-h158 are large proteins (203 kDa and 270 kDa, respectively) with intact Fc domains and have long biological half-lives in blood, which make them not well suited for clinical use as radioligands [29]. For example, RmAb158-scFv8D3 was radiolabeled with fluorine-18, and PET imaging was performed 12 h after injection, but it was not enough to detect differences between transgenic mice with A β deposits and wild-type mice [27]. For this reason, smaller recombinant formats without the Fc domain, such as TribodyTM (100 kDa) or di-scFv (58 kDa), have been created [28–30]. TribodyTM radioligand is composed of two fragments of mAb158 fused to Fab 8D3. It has a shorter half-life in blood than RmAb158-scFv8D3 and 8D3-F(ab')₂-h158 (9 h vs. 12 h and 19 h, respectively) and shown a clear distinction between wild-type and Alzheimer mouse models [27,28]. [^{124}I]I-Di-scFv3D6-8D3 was designed with an scFv derived from an anti-A β murine 3D6 antibody. It is capable of crossing the BBB and detecting *in vivo* intrabrain A β with better sensitivity than [^{11}C]PiB [29]. [^{125}I]I-Di-scFv3D6-8D3 has been measured at similar brain parenchymal concentrations as [^{125}I]I-mAb3D6-scFv8D3, but with less retention in the capillaries, probably due to the lower avidity of [^{125}I]I-Di-scFv3D6-8D3 against TfR. The elimination rate from the brain is similar for both [30]. Interestingly, a single domain shark antibody VNAR fragment (TXB2) with similar affinity to murine and human TfR1 was studied in PET because 3D8 is an antibody against murine TfR. It was fused to the A β antibody bapineuzumab (Bapi) and showed markedly increased brain uptake compared to Bapi alone [31]. Furthermore, a recent study with variants of the rat TfR antibody, OX26, chemically conjugated to F(ab')₂ fragments of Bapi has demonstrated that the TfR-mediated transport of an immunoPET radioligand enables sensitive imaging of brain

A β pathology in a rat model of AD (Figure 2C) [32]. In addition to beta-amyloidopathy, another proteinopathy, α -synuclein (α SYN) deposition, has been studied by immunoPET. Several radiolabeled bispecific antibodies were positively studied in an α SYN deposition model with PET, and the in vitro characterization showed that the antibodies had high sensitivity towards aggregated α SYN. However, the lack of signal in the transgenic models (L61 and A30P) could be due to the intracellular localization of the target [95]. Finally, an apolipoprotein E (ApoE)-derived brain shuttle peptide fused to an ^{18}F -labeled affibody against monomeric and oligomeric states of α SYN was successfully synthesized. The results of this study demonstrated that this strategy can potentially be utilized for brain molecular imaging [96].

ImmunoPET of neuroinflammation has been studied in the context of Alzheimer's disease. A bispecific antibody based on the triggering receptor expressed on myeloid cells 2 (TREM2), a marker of microglial activation, and 8D3 scFv against transferrin was radiolabeled with iodine-124. Radiolabeled mAb1729-scFv8D3_{CL} showed differences in ex vivo autoradiography but not in PET. Therefore, other antibody formats or high-affinity antibodies must be developed to obtain clear PET imaging [97].

Multiple sclerosis (MS) is an immune-mediated neurological disorder in which immunoPET has been used. Anti-CD20 mAb has shown promising results in patients with relapsing-remitting MS [98–100]. However, no clinical tool exists to evaluate whether there is a preferential benefit in patients with B-cell disease. Recently, two preclinical research studies aimed to develop antibody-based PET probes against CD20 [101,102]. In early research, [^{64}Cu]Cu-DOTA-rituximab showed human B cells in the spinal cord and brain of humanized autoimmune encephalomyelitis (EAE) mice model [101]. In the other study, ^{89}Zr -labeled-anti-CD20 mAb was injected subcutaneously or intravenously in EAE and control mice. Regardless of the route of administration, biodistribution to all major organs was consistent in EAE and control mice. However, initial tracer uptake was significantly higher in the draining lymph nodes and parts of the CNS when administered subcutaneously compared to intravenously in EAE mice [102].

6. Perspectives

The imaging diagnostic tools currently employed in neuro-oncology, computed tomography (CT) and magnetic resonance imaging (MRI), provide excellent anatomical information on the localization of brain lesions but are frequently not able to differentiate tumor tissue from other concurrent processes, such as inflammation, edema, or bleeding, resulting in under- or over-estimation of the actual extension of the tumor [81]. In addition, following radiation and/or chemotherapy, neuro-oncologists often encounter treatment-related changes, such as pseudoprogression or necrosis [103]. Another important issue in neuro-oncology is that the majority of GBM have gross tumor burden with an intact BBB that extends beyond the disrupted BBB. Therefore, successful treatment is only possible if an effective drug is delivered with adequate exposure to the entire population of targeted cells [90]. The development of new antibody-based PET probes that can cross the BBB could improve the diagnosis of brain tumors and also be a great tool for managing immune and radiation therapy.

Brain PET imaging allows a varied approach by assessing several physiopathological pathways, including neuroinflammation, neurotransmission, and protein aggregation, in neurological diseases [104]. Translocator protein-18 kDa (TSPO) is an 18 kDa outer mitochondrial membrane protein that is upregulated in neuroinflammation and a gold standard for PET imaging of activated microglia [105,106]. However, TSPO is expressed in reactive astrocytes, and many TSPO tracers have low sensitivity to the A147T variant. In addition, available TSPO ligands do not distinguish between pro- and anti-inflammatory microglia, which may be differentially expressed at the onset and progression of a neuroinflammatory condition [107,108]. Therefore, immunoPET could help develop new PET tracers targeting other neuroinflammatory biomarkers, such as a cannabinoid-2 receptor, purinergic receptors, or triggering receptors expressed on myeloid cells, among others [107]. Regarding

neurotransmission, immunoPET could allow the development of specific PET tracers for targets that have proven to be difficult using small molecules. For example, the possibility of obtaining *in vivo* information about the integrity of the cholinergic transmission by PET imaging is of major interest in studying the pathophysiology of various neurodegenerative disorders, such as Alzheimer's disease and Lewy body dementia, and has major relevance in cholinergic drug development [109]. Nevertheless, one of its key elements, muscarinic acetylcholine receptors (mAChRs), does not have a PET tracer with clinical applications, which demands mAChR tracers with improved imaging properties. In addition, M3 and M5 mAChR subtypes do not have any tracer in an early stage of development [110]. Finally, Parkinson's disease, a protein aggregation disease, remains a challenge because clinical features of the disease overlap with other neurodegenerative conditions, and diagnostic tests or biomarkers still do not allow for a definitive diagnosis from the earliest stages. In addition, there is a need to better define Parkinson's disease subtypes, which not only have different clinical presentations and prognoses but also differ in the underlying disease mechanisms, calling for personalized treatment approaches [111]. In this context, immunoPET could help create highly specific imaging probes against biomarkers, such as α SYN and TAR DNA-binding protein 43 (TDP-43), for which there are currently no other clinical PET probes available. It could improve early diagnosis and personalized medicine in neurodegenerative disorders.

Another field in which immunoPET could bring new perspectives is neuropsychiatry. No specific marker of a psychiatric disorder has been established thus far [112], and the development of antibody-based PET probes could help find them. For example, post-mortem investigations of GABA-A receptors in schizophrenia have shown that the α 1 subunit increases and the α 2 subunit decrease their expression, whereas the α 5 subunit has inconsistent results. However, the density of GABA-A receptors in schizophrenia does not appear to be abnormal in radioligand studies, as postmortem studies have demonstrated. Some authors and we believe that these negative findings can be explained by the lack of imaging tracers with high affinity and specificity for different subunits [113]. Therefore, the high specificity of antibodies could be used to detect each of the 19 subunits of GABA-A receptors. In this way, new immunoPET tools could be developed to look for new biomarkers in neuropsychiatric disorders.

Recently developed PET technologies, such as multiplexed PET (mPET), long axial field of view (LAFOV) PET/CT scanners, and hybrid PET/MR imaging, together with immunoPET probes, could lead to novel knowledge in CNS research and contribute to drug development. The use of mPET, which can detect two radioisotopes at the same time [114], could allow the differentiation of, for example, specific GABA-A receptor configurations, such as α 1 β 2 or α 1 β 3 subunits, at once. This information could give a better picture of the GABA-A receptor subtype expression *in vivo* in psychiatric disorders. LAFOV PET scanners have an extended axial FOV (> 1 m), enabling whole-body dynamic PET imaging, and have several benefits, such as increased sensitivity, whole-body kinetic analysis, and lower radiotracer dosing [115,116]. These devices allow physiological or pathophysiological brain–heart–kidney–liver–gut interactions to be studied [115]. Finally, hybrid PET/MR allows temporal and spatial matching datasets displaying different physiological and metabolic information about a disease process. This multimodal technology could provide an efficient means for acquiring images in neuro-oncology, neurodegenerative disease, epilepsy, cerebrovascular disease, psychiatry, and neurology and may show added benefit beyond separate acquisition and interpretation of PET and MRI alone [117].

Current advances in antibody engineering have achieved successful application of immunoPET to the brain. This achievement opens the doors to improving diagnosis and treatment in neuro-oncology, neurology, and neuropsychiatry.

Author Contributions: All authors contributed to the original draft preparation and reviewed and edited the manuscript. All authors have read and agreed to the published version of the manuscript.

Funding: This paper was supported by the European Union’s Horizon 2020 research and innovation program under the Marie Skłodowska-Curie (grant 891455) and the Turku University Hospital (grant 11135).

Conflicts of Interest: The authors declare that the research was conducted in the absence of any commercial or financial relationships that could be construed as a potential conflict of interest.

References

1. Marik, J.; Junutula, J.R. Emerging role of immunoPET in receptor targeted cancer therapy. *Curr. Drug Deliv.* **2011**, *8*, 70–78. [[CrossRef](#)] [[PubMed](#)]
2. Fu, R.; Carroll, L.; Yahioğlu, G.; Aboagye, E.O.; Miller, P.W. Antibody Fragment and Affibody ImmunoPET Imaging Agents: Radiolabelling Strategies and Applications. *ChemMedChem* **2018**, *13*, 2466–2478. [[CrossRef](#)] [[PubMed](#)]
3. Wu, A.M.; Olafsen, T. Antibodies for molecular imaging of cancer. *Cancer J.* **2008**, *14*, 191–197. [[CrossRef](#)] [[PubMed](#)]
4. Goldenberg, D.M.; Nabi, H.A. Breast cancer imaging with radiolabeled antibodies. *Semin. Nucl. Med.* **1999**, *29*, 41–48. [[CrossRef](#)] [[PubMed](#)]
5. McCabe, K.E.; Wu, A.M. Positive progress in immunoPET—not just a coincidence. *Cancer Biother. Radiopharm.* **2010**, *25*, 253–261. [[CrossRef](#)] [[PubMed](#)]
6. Sehlin, D.; Syvänen, S.; Ballanger, B.; Barthel, H.; Bischof, G.N.; Boche, D.; Boecker, H.; Bohn, K.P.; Borghammer, P.; Cross, D.; et al. Engineered antibodies: New possibilities for brain PET? *Eur. J. Nucl. Med. Mol. Imaging* **2019**, *46*, 2848–2858. [[CrossRef](#)]
7. Mäger, I.; Meyer, A.H.; Li, J.; Lenter, M.; Hildebrandt, T.; Leparç, G.; Wood, M.J. Targeting blood-brain-barrier transcytosis—perspectives for drug delivery. *Neuropharmacology* **2017**, *120*, 4–7. [[CrossRef](#)]
8. Banks, W.A.; Terrell, B.; Farr, S.A.; Robinson, S.M.; Nonaka, N.; Morley, J.E. Passage of amyloid beta protein antibody across the blood-brain barrier in a mouse model of Alzheimer’s disease. *Peptides* **2002**, *23*, 2223–2226. [[CrossRef](#)]
9. Mach, R.H.; Schwarz, S.W. Challenges for Developing PET Tracers: Isotopes, Chemistry, and Regulatory Aspects. *PET Clin.* **2010**, *5*, 131–153. [[CrossRef](#)]
10. Pike, V.W. PET radiotracers: Crossing the blood-brain barrier and surviving metabolism. *Trends Pharmacol. Sci.* **2009**, *30*, 431–440. [[CrossRef](#)]
11. Ruiz-López, E.; Calatayud-Pérez, J.; Castells-Yus, I.; Gimeno-Peribáñez, M.J.; Mendoza-Calvo, N.; Morcillo, M.; Schuhmacher, A.J. Diagnosis of Glioblastoma by Immuno-Positron Emission Tomography. *Cancers* **2021**, *14*, 74. [[CrossRef](#)] [[PubMed](#)]
12. McLean, D.; Cooke, M.J.; Albay, R.; Glabe, C.; Shoichet, M.S. Positron emission tomography imaging of fibrillar parenchymal and vascular amyloid- β in TgCRND8 mice. *ACS Chem. Neurosci.* **2013**, *4*, 613–623. [[CrossRef](#)] [[PubMed](#)]
13. McLean, D.; Cooke, M.J.; Wang, Y.; Green, D.; Fraser, P.E.; George-Hyslop, P.S.; Shoichet, M.S. Anti-amyloid- β -mediated positron emission tomography imaging in Alzheimer’s disease mouse brains. *PLoS ONE* **2012**, *7*, e51958. [[CrossRef](#)] [[PubMed](#)]
14. Hervé, F.; Ghinea, N.; Scherrmann, J.M. CNS delivery via adsorptive transcytosis. *AAPS J.* **2008**, *10*, 455–472. [[CrossRef](#)] [[PubMed](#)]
15. Li, T.; Bourgeois, J.-P.; Celli, S.; Glacial, F.; Le Sourd, A.-M.; Mecheri, S.; Weksler, B.; Romero, I.; Couraud, P.-O.; Rougeon, F.; et al. Cell-penetrating anti-GFAP VHH and corresponding fluorescent fusion protein VHH-GFP spontaneously cross the blood-brain barrier and specifically recognize astrocytes: Application to brain imaging. *FASEB J.* **2012**, *26*, 3969–3979. [[CrossRef](#)] [[PubMed](#)]
16. Li, T.; Vandesquille, M.; Koukouli, F.; Duffeffant, C.; Youssef, I.; Lenormand, P.; Ganneau, C.; Maskos, U.; Czech, C.; Grueninger, F. Camelid single-domain antibodies: A versatile tool for in vivo imaging of extracellular and intracellular brain targets. *J. Control. Release* **2016**, *243*, 1–10. [[CrossRef](#)]
17. Terstappen, G.C.; Meyer, A.H.; Bell, R.D.; Zhang, W. Strategies for delivering therapeutics across the blood-brain barrier. *Nat. Rev. Drug Discov.* **2021**, *20*, 362–383. [[CrossRef](#)]
18. Pulgar, V.M. Transcytosis to Cross the Blood Brain Barrier, New Advancements and Challenges. *Front. Neurosci.* **2018**, *12*, 1019. [[CrossRef](#)]
19. Kouhi, A.; Pachipulusu, V.; Kapenstein, T.; Hu, P.; Epstein, A.L.; Khawli, L.A. Brain Disposition of Antibody-Based Therapeutics: Dogma, Approaches and Perspectives. *Int. J. Mol. Sci.* **2021**, *22*, 6442. [[CrossRef](#)]
20. Yu, Y.J.; Zhang, Y.; Kenrick, M.; Hoyte, K.; Luk, W.; Lu, Y.; Atwal, J.; Elliott, J.M.; Prabhu, S.; Watts, R.J.; et al. Boosting brain uptake of a therapeutic antibody by reducing its affinity for a transcytosis target. *Sci. Transl. Med.* **2011**, *3*, 84ra44. [[CrossRef](#)]
21. Niewoehner, J.; Bohrmann, B.; Collin, L.; Urich, E.; Sade, H.; Maier, P.; Rueger, P.; Stracke, J.O.; Lau, W.; Tissot, A.C.; et al. Increased brain penetration and potency of a therapeutic antibody using a monovalent molecular shuttle. *Neuron* **2014**, *81*, 49–60. [[CrossRef](#)] [[PubMed](#)]
22. Sehlin, D.; Fang, X.T.; Cato, L.; Antoni, G.; Lannfelt, L.; Syvänen, S. Antibody-based PET imaging of amyloid beta in mouse models of Alzheimer’s disease. *Nat. Commun.* **2016**, *7*, 10759. [[CrossRef](#)] [[PubMed](#)]
23. Sehlin, D.; Fang, X.T.; Meier, S.R.; Jansson, M.; Syvänen, S. Pharmacokinetics, biodistribution and brain retention of a bispecific antibody-based PET radioligand for imaging of amyloid- β . *Sci. Rep.* **2017**, *7*, 17254. [[CrossRef](#)] [[PubMed](#)]
24. Hultqvist, G.; Syvänen, S.; Fang, X.T.; Lannfelt, L.; Sehlin, D. Bivalent Brain Shuttle Increases Antibody Uptake by Monovalent Binding to the Transferrin Receptor. *Theranostics* **2017**, *7*, 308–318. [[CrossRef](#)] [[PubMed](#)]

25. Meier, S.R.; Syvänen, S.; Hultqvist, G.; Fang, X.T.; Roshanbin, S.; Lannfelt, L.; Neumann, U.; Sehlin, D. Antibody-Based In Vivo PET Imaging Detects Amyloid- β Reduction in Alzheimer Transgenic Mice After BACE-1 Inhibition. *J. Nucl. Med.* **2018**, *59*, 1885–1891. [[CrossRef](#)] [[PubMed](#)]
26. Meier, S.R.; Sehlin, D.; Roshanbin, S.; Falk, V.L.; Saito, T.; Saido, T.C.; Neumann, U.; Rokka, J.; Eriksson, J.; Syvänen, S. (11)C-PiB and (124)I-Antibody PET Provide Differing Estimates of Brain Amyloid- β After Therapeutic Intervention. *J. Nucl. Med.* **2022**, *63*, 302–309. [[CrossRef](#)] [[PubMed](#)]
27. Syvänen, S.; Fang, X.T.; Faresjö, R.; Rokka, J.; Lannfelt, L.; E Olberg, D.; Eriksson, J.; Sehlin, D. Fluorine-18-Labeled Antibody Ligands for PET Imaging of Amyloid- β in Brain. *ACS Chem. Neurosci.* **2020**, *11*, 4460–4468. [[CrossRef](#)]
28. Syvänen, S.; Fang, X.T.; Hultqvist, G.; Meier, S.R.; Lannfelt, L.; Sehlin, D. A bispecific Tribody PET radioligand for visualization of amyloid-beta protofibrils—A new concept for neuroimaging. *Neuroimage* **2017**, *148*, 55–63. [[CrossRef](#)]
29. Fang, X.T.; Hultqvist, G.; Meier, S.R.; Antoni, G.; Sehlin, D.; Syvänen, S. High detection sensitivity with antibody-based PET radioligand for amyloid beta in brain. *Neuroimage* **2019**, *184*, 881–888. [[CrossRef](#)]
30. Faresjö, R.; Bonvicini, G.; Fang, X.T.; Aguilar, X.; Sehlin, D.; Syvänen, S. Brain pharmacokinetics of two BBB penetrating bispecific antibodies of different size. *Fluids Barriers CNS* **2021**, *18*, 26. [[CrossRef](#)]
31. Sehlin, D.; Stocki, P.; Gustavsson, T.; Hultqvist, G.; Walsh, F.S.; Rutkowski, J.L.; Syvänen, S. Brain delivery of biologics using a cross-species reactive transferrin receptor 1 VNAR shuttle. *FASEB J.* **2020**, *34*, 13272–13283. [[CrossRef](#)] [[PubMed](#)]
32. Bonvicini, G.; Syvänen, S.; Andersson, K.G.; Haaparanta-Solin, M.; López-Picón, F.; Sehlin, D. ImmunoPET imaging of amyloid-beta in a rat model of Alzheimer’s disease with a bispecific, brain-penetrating fusion protein. *Transl. Neurodegener.* **2022**, *11*, 55. [[CrossRef](#)] [[PubMed](#)]
33. Neuwelt, E.A.; Diehl, J.T.; Vu, L.H.; Hill, S.A.; Michael, A.J.; Frenkel, E.P. Monitoring of methotrexate delivery in patients with malignant brain tumors after osmotic blood-brain barrier disruption. *Ann. Intern. Med.* **1981**, *94*, 449–454. [[CrossRef](#)]
34. Arif, W.M.; Elsinga, P.H.; Gasca-Salas, C.; Versluis, M.; Martínez-Fernández, R.; Dierckx, R.A.; Borra, R.J.; Luurtsema, G. Focused ultrasound for opening blood-brain barrier and drug delivery monitored with positron emission tomography. *J. Control. Release* **2020**, *324*, 303–316. [[CrossRef](#)] [[PubMed](#)]
35. Leinenga, G.; Bodea, L.G.; Koh, W.K.; Nisbet, R.M.; Götz, J. Delivery of Antibodies into the Brain Using Focused Scanning Ultrasound. *J. Vis. Exp.* **2020**, *161*, e61372. [[CrossRef](#)]
36. Arvanitis, C.D.; Askoxylakis, V.; Guo, Y.; Datta, M.; Kloepper, J.; Ferraro, G.B.; Bernabeu, M.O.; Fukumura, D.; McDannold, N.; Jain, R.K. Mechanisms of enhanced drug delivery in brain metastases with focused ultrasound-induced blood-tumor barrier disruption. *Proc. Natl. Acad. Sci. USA* **2018**, *115*, E8717–E8726. [[CrossRef](#)]
37. Tran, V.L.; Novell, A.; Tournier, N.; Gerstenmayer, M.; Schweitzer-Chaput, A.; Mateos, C.; Jegou, B.; Bouleau, A.; Nozach, H.; Winkeler, A.; et al. Impact of blood-brain barrier permeabilization induced by ultrasound associated to microbubbles on the brain delivery and kinetics of cetuximab: An immunoPET study using. *J. Control. Release* **2020**, *328*, 304–312. [[CrossRef](#)] [[PubMed](#)]
38. Sheybani, N.; Breza, V.; Paul, S.; McCauley, K.; Berr, S.; Miller, W.; Neumann, K.; Price, R. ImmunoPET-informed sequence for focused ultrasound-targeted mCD47 blockade controls glioma. *J. Control. Release* **2021**, *331*, 19–29. [[CrossRef](#)] [[PubMed](#)]
39. Poduslo, J.F.; Curran, G.L.; Berg, C.T. Macromolecular permeability across the blood-nerve and blood-brain barriers. *Proc. Natl. Acad. Sci. USA* **1994**, *91*, 5705–5709. [[CrossRef](#)] [[PubMed](#)]
40. Spiess, C.; Zhai, Q.; Carter, P.J. Alternative molecular formats and therapeutic applications for bispecific antibodies. *Mol. Immunol.* **2015**, *67*, 95–106. [[CrossRef](#)]
41. Merchant, A.M.; Zhu, Z.; Yuan, J.Q.; Goddard, A.; Adams, C.W.; Presta, L.G.; Carter, P. An efficient route to human bispecific IgG. *Nat. Biotechnol.* **1998**, *16*, 677–681. [[CrossRef](#)] [[PubMed](#)]
42. Schaefer, W.; Regula, J.T.; Böhner, M.; Schanzer, J.; Croasdale, R.; Dürr, H.; Gassner, C.; Georges, G.; Kettenberger, H.; Imhof-Jung, S.; et al. Immunoglobulin domain crossover as a generic approach for the production of bispecific IgG antibodies. *Proc. Natl. Acad. Sci. USA* **2011**, *108*, 11187–11192. [[CrossRef](#)] [[PubMed](#)]
43. Lewis, S.M.; Wu, X.; Pustilnik, A.; Sereno, A.; Huang, F.; Rick, H.L.; Guntas, G.; Leaver-Fay, A.; Smith, E.M.; Ho, C.; et al. Generation of bispecific IgG antibodies by structure-based design of an orthogonal Fab interface. *Nat. Biotechnol.* **2014**, *32*, 191–198. [[CrossRef](#)] [[PubMed](#)]
44. Coloma, M.J.; Morrison, S.L. Design and production of novel tetravalent bispecific antibodies. *Nat. Biotechnol.* **1997**, *15*, 159–163. [[CrossRef](#)] [[PubMed](#)]
45. Yazaki, P.J.; Lee, B.; Channappa, D.; Cheung, C.W.; Crow, D.; Chea, J.; Poku, E.; Li, L.; Andersen, J.T.; Sandlie, I.; et al. A series of anti-CEA/anti-DOTA bispecific antibody formats evaluated for pre-targeting: Comparison of tumor uptake and blood clearance. *Protein Eng. Des. Sel.* **2013**, *26*, 187–193. [[CrossRef](#)]
46. Mallender, W.D.; Voss, E.W., Jr. Construction, expression, and activity of a bivalent bispecific single-chain antibody. *J. Biol. Chem.* **1994**, *269*, 199–206. [[CrossRef](#)]
47. Wolf, E.; Hofmeister, R.; Kufer, P.; Schlereth, B.; Baeuerle, P.A. BiTEs: Bispecific antibody constructs with unique anti-tumor activity. *Drug Discov. Today* **2005**, *10*, 1237–1244. [[CrossRef](#)]
48. Kariolis, M.S.; Wells, R.C.; Getz, J.A.; Kwan, W.; Mahon, C.S.; Tong, R.; Kim, D.J.; Srivastava, A.; Bedard, C.; Henne, K.R.; et al. Brain delivery of therapeutic proteins using an Fc fragment blood-brain barrier transport vehicle in mice and monkeys. *Sci. Transl. Med.* **2020**, *12*, eaay1359. [[CrossRef](#)]

49. Meier, S.R.; Sehlin, D.; Syvänen, S. Passive and receptor mediated brain delivery of an anti-GFAP nanobody. *Nucl. Med. Biol.* **2022**, *114–115*, 128–134. [[CrossRef](#)]
50. Vorobyeva, A.; Schulga, A.; Konovalova, E.; Mitran, B.; Garousi, J.; Rinne, S.; Orlova, A.; Deyev, S.; Tolmachev, V. Comparison of tumor-targeting properties of directly and indirectly radioiodinated designed ankyrin repeat protein (DARPin) G3 variants for molecular imaging of HER2. *Int. J. Oncol.* **2019**, *54*, 1209–1220. [[CrossRef](#)]
51. Brinkmann, U.; Kontermann, R.E. The making of bispecific antibodies. *MAbs* **2017**, *9*, 182–212. [[CrossRef](#)] [[PubMed](#)]
52. Liu, L. Pharmacokinetics of monoclonal antibodies and Fc-fusion proteins. *Protein Cell* **2018**, *9*, 15–32. [[CrossRef](#)] [[PubMed](#)]
53. Mammen, M.; Choi, S.K.; Whitesides, G.M. Polyvalent Interactions in Biological Systems: Implications for Design and Use of Multivalent Ligands and Inhibitors. *Angew. Chem. Int. Ed. Engl.* **1998**, *37*, 2754–2794. [[CrossRef](#)]
54. Datta-Mannan, A.; Brown, R.M.; Fitchett, J.; Heng, A.R.; Balasubramaniam, D.; Pereira, J.; Croy, J.E. Modulation of the Biophysical Properties of Bifunctional Antibodies as a Strategy for Mitigating Poor Pharmacokinetics. *Biochemistry* **2019**, *58*, 3116–3132. [[CrossRef](#)] [[PubMed](#)]
55. Shukla, A.K.; Kumar, U. Positron emission tomography: An overview. *J. Med. Phys.* **2006**, *31*, 13–21. [[CrossRef](#)] [[PubMed](#)]
56. Wu, A.M. Antibodies and antimatter: The resurgence of immuno-PET. *J. Nucl. Med.* **2009**, *50*, 2–5. [[CrossRef](#)] [[PubMed](#)]
57. Conti, M.; Eriksson, L. Physics of pure and non-pure positron emitters for PET: A review and a discussion. *EJNMMI Phys.* **2016**, *3*, 8. [[CrossRef](#)] [[PubMed](#)]
58. Bunka, M.; Müller, C.; Vermeulen, C.; Haller, S.; Türler, A.; Schibli, R.; van der Meulen, N.P. Imaging quality of (44)Sc in comparison with five other PET radionuclides using Derenzo phantoms and preclinical PET. *Appl. Radiat. Isot.* **2016**, *110*, 129–133. [[CrossRef](#)]
59. Kręcis, P.; Czarnecka, K.; Królicki, L.; Mikiciuk-Olasik, E.; Szymański, P. Radiolabeled Peptides and Antibodies in Medicine. *Bioconjug Chem.* **2021**, *32*, 25–42. [[CrossRef](#)]
60. Oroujeni, M.; Garousi, J.; Andersson, K.G.; Löfblom, J.; Mitran, B.; Orlova, A.; Tolmachev, V. Preclinical Evaluation of [68Ga]Ga-DFO-ZEGFR:2377: A Promising Affibody-Based Probe for Noninvasive PET Imaging of EGFR Expression in Tumors. *Cells* **2018**, *7*, 141. [[CrossRef](#)]
61. Chakravarty, R.; Goel, S.; Valdovinos, H.F.; Hernandez, R.; Hong, H.; Nickles, R.J.; Cai, W. Matching the decay half-life with the biological half-life: ImmunoPET imaging with ⁴⁴Sc-labeled cetuximab Fab fragment. *Bioconjug. Chem.* **2014**, *25*, 2197–2204. [[CrossRef](#)] [[PubMed](#)]
62. Stéen, E.J.L.; Edem, P.E.; Nørregaard, K.; Jørgensen, J.T.; Shalgunov, V.; Kjaer, A.; Herth, M.M. Pretargeting in nuclear imaging and radionuclide therapy: Improving efficacy of theranostics and nanomedicines. *Biomaterials* **2018**, *179*, 209–245. [[CrossRef](#)] [[PubMed](#)]
63. Rossin, R.; Verkerk, P.R.; Bosch, S.M.V.D.; Vulderson, R.C.M.; Verel, I.; Lub, J.; Robillard, M.S. In vivo chemistry for pretargeted tumor imaging in live mice. *Angew. Chem. Int. Ed. Engl.* **2010**, *49*, 3375–3378. [[CrossRef](#)] [[PubMed](#)]
64. Carroll, L.; Evans, H.L.; Aboagye, E.O.; Spivey, A.C. Bioorthogonal chemistry for pre-targeted molecular imaging—progress and prospects. *Org. Biomol. Chem.* **2013**, *11*, 5772–5781. [[CrossRef](#)] [[PubMed](#)]
65. Oliveira, B.L.; Guo, Z.; Bernardes, G.J.L. Inverse electron demand Diels-Alder reactions in chemical biology. *Chem. Soc. Rev.* **2017**, *46*, 4895–4950. [[CrossRef](#)]
66. Poulie, C.B.; Jørgensen, J.T.; Shalgunov, V.; Kougioumtzoglou, G.; Jeppesen, T.E.; Kjaer, A.; Herth, M.M. Evaluation of [⁶⁴Cu]Cu-NOTA-PEG₇-H-Tz for Pretargeted Imaging in LS174T Xenografts-Comparison to [¹¹¹In]In-DOTA-PEG₁₁-BisPy-Tz. *Molecules* **2021**, *26*, 544. [[CrossRef](#)]
67. Stéen, E.J.L.; Jørgensen, J.T.; Denk, C.; Battisti, U.M.; Nørregaard, K.; Edem, P.E.; Bratteby, K.; Shalgunov, V.; Wilkovitsch, M.; Svatunek, D.; et al. Lipophilicity and Click Reactivity Determine the Performance of Bioorthogonal Tetrazine Tools in Pretargeted In Vivo Chemistry. *ACS Pharmacol. Transl. Sci.* **2021**, *4*, 824–833. [[CrossRef](#)]
68. Shalgunov, V.; Broek, S.L.v.D.; Andersen, I.V.; Vázquez, R.G.; Raval, N.R.; Palner, M.; Mori, Y.; Schäfer, G.; Herrmann, B.; Mikula, H.; et al. Pretargeted imaging beyond the blood–brain barrier-Utopia or Feasible? *Pharmaceuticals (Basel)* **2022**, *15*, 1191.
69. Dijkers, E.C.; Oude Munnink, T.H.; Kosterink, J.G.; Brouwers, A.H.; Jager, P.L.; De Jong, J.R.; Van Dongen, G.A.; Schroder, C.P.; Lub-de Hooge, M.N.; de Vries, E.G. Biodistribution of ⁸⁹Zr-trastuzumab and PET imaging of HER2-positive lesions in patients with metastatic breast cancer. *Clin. Pharmacol. Ther.* **2010**, *87*, 586–592. [[CrossRef](#)]
70. Ulaner, G.A.; Lyashchenko, S.K.; Riedl, C.; Ruan, S.; Zanzonico, P.B.; Lake, D.; Jhaveri, K.; Zeglis, B.; Lewis, J.S.; O'Donoghue, J.A. First-in-Human Human Epidermal Growth Factor Receptor 2-Targeted Imaging Using ⁸⁹Zr-Pertuzumab PET/CT: Dosimetry and Clinical Application in Patients with Breast Cancer. *J. Nucl. Med.* **2018**, *59*, 900–906. [[CrossRef](#)]
71. Rousseau, C.; Goldenberg, D.; Colombié, M.; Sébille, J.-C.; Meingan, P.; Ferrer, L.; Baumgartner, P.; Cerato, E.; Masson, D.; Campone, M.; et al. Initial Clinical Results of a Novel Immuno-PET Theranostic Probe in Human Epidermal Growth Factor Receptor 2-Negative Breast Cancer. *J. Nucl. Med.* **2020**, *61*, 1205–1211. [[CrossRef](#)] [[PubMed](#)]
72. Zhou, Z.; McDougald, D.; Meshaw, R.; Balyasnikova, I.; Zalutsky, M.R.; Vaidyanathan, G. Labeling single domain antibody fragments with (18)F using a novel residualizing prosthetic agent-N-succinimidyl 3-(1-(2-(2-(2-[(18)F]fluoroethoxy)ethoxy)ethoxy)ethyl)-1H-1,2,3-triazol-4-yl)-5-(guanidinomethyl)benzoate. *Nucl. Med. Biol.* **2021**, *100–101*, 24–35. [[CrossRef](#)] [[PubMed](#)]
73. Chen, W. Clinical applications of PET in brain tumors. *J. Nucl. Med.* **2007**, *48*, 1468–1481. [[CrossRef](#)] [[PubMed](#)]
74. Cai, W.; Wu, Y.; Chen, K.; Cao, Q.; Tice, D.A.; Chen, X. In vitro and in vivo characterization of ⁶⁴Cu-labeled Abegrin, a humanized monoclonal antibody against integrin alpha v beta 3. *Cancer Res.* **2006**, *66*, 9673–9681. [[CrossRef](#)] [[PubMed](#)]

75. Luo, H.; Hernandez, R.; Hong, H.; Graves, S.A.; Yang, Y.; England, C.G.; Theuer, C.P.; Nickles, R.J.; Cai, W. Noninvasive brain cancer imaging with a bispecific antibody fragment, generated via click chemistry. *Proc. Natl. Acad. Sci. USA* **2015**, *112*, 12806–12811. [[CrossRef](#)] [[PubMed](#)]
76. Tang, Y.; Hu, Y.; Liu, W.; Chen, L.; Zhao, Y.; Ma, H.; Yang, J.; Yang, Y.; Liao, J.; Cai, J.; et al. A radiopharmaceutical [⁸⁹Zr]Zr-DFO-nimotuzumab for immunoPET with epidermal growth factor receptor expression in vivo. *Nucl. Med. Biol.* **2019**, *70*, 23–31. [[CrossRef](#)]
77. Zhou, B.; Wang, H.; Liu, R.; Wang, M.; Deng, H.; Giglio, B.C.; Gill, P.S.; Shan, H.; Li, Z. PET Imaging of Dll4 Expression in Glioblastoma and Colorectal Cancer Xenografts Using (64)Cu-Labeled Monoclonal Antibody 61B. *Mol. Pharm.* **2015**, *12*, 3527–3534. [[CrossRef](#)]
78. Pandya, D.; Sinha, A.; Yuan, H.; Mutkus, L.; Stumpf, K.; Marini, F.; Wadas, T. Imaging of Fibroblast Activation Protein Alpha Expression in a Preclinical Mouse Model of Glioma Using Positron Emission Tomography. *Molecules* **2020**, *25*, 3672. [[CrossRef](#)]
79. Hernandez, R.; Sun, H.; England, C.G.; Valdovinos, H.F.; Barnhart, T.E.; Yang, Y.; Cai, W. ImmunoPET Imaging of CD146 Expression in Malignant Brain Tumors. *Mol. Pharm.* **2016**, *13*, 2563–2570. [[CrossRef](#)]
80. Yang, Y.; Hernandez, R.; Rao, J.; Yin, L.; Qu, Y.; Wu, J.; England, C.G.; Graves, S.A.; Lewis, C.M.; Wang, P.; et al. Targeting CD146 with a ⁶⁴Cu-labeled antibody enables in vivo immunoPET imaging of high-grade gliomas. *Proc. Natl. Acad. Sci. USA* **2015**, *112*, E6525–E6534. [[CrossRef](#)]
81. De Lucas, A.G.; Schuhmacher, A.J.; Oteo, M.; Romero, E.; Cámara, J.A.; de Martino, A.; Arroyo, A.G.; Morcillo, M.Á.; Squatrito, M.; Martínez-Torrecuadrada, J.L.; et al. Targeting MT1-MMP as an ImmunoPET-Based Strategy for Imaging Gliomas. *PLoS ONE* **2016**, *11*, e0158634. [[CrossRef](#)] [[PubMed](#)]
82. Nigam, S.; McCarl, L.; Kumar, R.; Edinger, R.S.; Kurland, B.F.; Anderson, C.J.; Panigrahy, A.; Kohanbash, G.; Edwards, W.B. Preclinical ImmunoPET Imaging of Glioblastoma-Infiltrating Myeloid Cells Using Zirconium-89 Labeled Anti-CD11b Antibody. *Mol. Imaging Biol.* **2020**, *22*, 685–694. [[CrossRef](#)] [[PubMed](#)]
83. Jansen, M.H.; Lagerweij, T.; Sewing, A.C.P.; Vugts, D.J.; van Vuurden, D.G.; Molthoff, C.F.; Caretti, V.; Veringa, S.J.; Petersen, N.; Carcaboso, A.M.; et al. Bevacizumab Targeting Diffuse Intrinsic Pontine Glioma: Results of ⁸⁹Zr-Bevacizumab PET Imaging in Brain Tumor Models. *Mol. Cancer Ther.* **2016**, *15*, 2166–2174. [[CrossRef](#)] [[PubMed](#)]
84. Jansen, M.H.; van Zanten, S.E.M.V.; van Vuurden, D.G.; Huisman, M.C.; Vugts, D.J.; Hoekstra, O.S.; van Dongen, G.A.; Kaspers, G.-J.L. Molecular Drug Imaging: (89)Zr-Bevacizumab PET in Children with Diffuse Intrinsic Pontine Glioma. *J. Nucl. Med.* **2017**, *58*, 711–716. [[CrossRef](#)] [[PubMed](#)]
85. Van Zanten, S.E.V.; Sewing, A.C.P.; Van Lingen, A.; Hoekstra, O.S.; Wesseling, P.; Meel, M.H.; Van Vuurden, D.G.; Kaspers, G.J.; Hulleman, E.; Bugiani, M. Multiregional Tumor Drug-Uptake Imaging by PET and Microvascular Morphology in End-Stage Diffuse Intrinsic Pontine Glioma. *J. Nucl. Med.* **2018**, *59*, 612–615. [[CrossRef](#)] [[PubMed](#)]
86. den Hollander, M.W.; Bensch, F.; Glaudemans, A.W.; Munnink, T.H.O.; Enting, R.H.; den Dunnen, W.F.; Heesters, M.A.; Kruijff, F.A.; Lub-de Hooge, M.N.; de Groot, J.C.; et al. TGF-β Antibody Uptake in Recurrent High-Grade Glioma Imaged with ⁸⁹Zr-Fresolimumab PET. *J. Nucl. Med.* **2015**, *56*, 1310–1314. [[CrossRef](#)] [[PubMed](#)]
87. Gonzalez-Junca, A.; Reiners, O.; Borrero-Garcia, L.D.; Beckford-Vera, D.; Lazar, A.A.; Chou, W.; Braunstein, S.; VanBrocklin, H.; Franc, B.L.; Barcellos-Hoff, M.H. Positron Emission Tomography Imaging of Functional Transforming Growth Factor β (TGFβ) Activity and Benefit of TGFβ Inhibition in Irradiated Intracranial Tumors. *Int J Radiat Oncol Biol Phys.* **2021**, *109*, 527–539. [[CrossRef](#)]
88. Krebs, S.; Grommes, C.; McDevitt, M.R.; Carlin, S.D.; O'Donoghue, J.A.; Graham, M.S.; Young, R.J.; Schöder, H.; Gutin, P.H.; Bander, N.H.; et al. [⁸⁹Zr]Zr-huJ591 immuno-PET targeting PSMA in IDH mutant anaplastic oligodendroglioma. *Eur. J. Nucl. Med. Mol. Imaging* **2022**, *49*, 783–785. [[CrossRef](#)]
89. Matsuda, M.; Ishikawa, E.; Yamamoto, T.; Hatano, K.; Joraku, A.; Iizumi, Y.; Masuda, Y.; Nishiyama, H.; Matsumura, A. Potential use of prostate specific membrane antigen (PSMA) for detecting the tumor neovasculature of brain tumors by PET imaging with ⁸⁹Zr-Df-IAB2M anti-PSMA minibody. *J. Neurooncol.* **2018**, *138*, 581–589. [[CrossRef](#)]
90. Sarkaria, J.N.; Hu, L.S.; Parney, I.F.; Pafundi, D.H.; Brinkmann, D.H.; Laack, N.N.; Giannini, C.; Burns, T.C.; Kizilbash, S.; Laramy, J.K.; et al. Is the blood-brain barrier really disrupted in all glioblastomas? A critical assessment of existing clinical data. *Neuro Oncol.* **2018**, *20*, 184–191. [[CrossRef](#)]
91. Zaky, W.; Wellner, M.; Brown, R.J.; Blüml, S.; Finlay, J.L.; Dhall, G. Treatment of children with diffuse intrinsic pontine gliomas with chemoradiotherapy followed by a combination of temozolomide, irinotecan, and bevacizumab. *Pediatr. Hematol. Oncol.* **2013**, *30*, 623–632. [[CrossRef](#)] [[PubMed](#)]
92. Aguilera, D.G.; Mazewski, C.; Hayes, L.; Jordan, C.; Esiashvilli, N.; Janns, A.; MacDonald, T.J. Prolonged survival after treatment of diffuse intrinsic pontine glioma with radiation, temozolamide, and bevacizumab: Report of 2 cases. *J. Pediatr. Hematol. Oncol.* **2013**, *35*, e42–6. [[CrossRef](#)] [[PubMed](#)]
93. Fissers, J.; Waldron, A.-M.; De Vijlder, T.; Van Broeck, B.; Pemberton, D.J.; Mercken, M.; Van Der Veken, P.; Joossens, J.; Augustyns, K.; Dedeurwaerdere, S.; et al. Synthesis and Evaluation of a Zr-89-Labeled Monoclonal Antibody for Immuno-PET Imaging of Amyloid-β Deposition in the Brain. *Mol. Imaging Biol.* **2016**, *18*, 598–605. [[CrossRef](#)] [[PubMed](#)]

94. Magnusson, K.; Sehlin, D.; Syvänen, S.; Svedberg, M.M.; Philipson, O.; Söderberg, L.; Tegerstedt, K.; Holmquist, M.; Gellerfors, P.; Tolmachev, V.; et al. Specific uptake of an amyloid- β protofibril-binding antibody-tracer in A β PP transgenic mouse brain. *J. Alzheimers Dis.* **2013**, *37*, 29–40. [[CrossRef](#)]
95. Roshanbin, S.; Xiong, M.; Hultqvist, G.; Söderberg, L.; Zachrisson, O.; Meier, S.; Ekmark-Lewén, S.; Bergström, J.; Ingelsson, M.; Sehlin, D.; et al. In vivo imaging of alpha-synuclein with antibody-based PET. *Neuropharmacology* **2022**, *208*, 108985. [[CrossRef](#)] [[PubMed](#)]
96. Morito, T.; Harada, R.; Iwata, R.; Du, Y.; Okamura, N.; Kudo, Y.; Yanai, K. Synthesis and pharmacokinetic characterisation of a fluorine-18 labelled brain shuttle peptide fusion dimeric affibody. *Sci. Rep.* **2021**, *11*, 2588. [[CrossRef](#)] [[PubMed](#)]
97. Meier, S.R.; Sehlin, D.; Hultqvist, G.; Syvänen, S. Pinpointing Brain TREM2 Levels in Two Mouse Models of Alzheimer's Disease. *Mol. Imaging Biol.* **2021**, *23*, 665–675. [[CrossRef](#)] [[PubMed](#)]
98. Bar-Or, A.; Calabresi, P.A.J.; Arnold, D.; Markowitz, C.; Shafer, S.; Kasper, L.H.; Waubant, E.; Gazda, S.; Fox, R.J.; Panzara, M.; et al. Rituximab in relapsing-remitting multiple sclerosis: A 72-week, open-label, phase I trial. *Ann Neurol.* **2008**, *63*, 395–400. [[CrossRef](#)] [[PubMed](#)]
99. Bar-Or, A.; Grove, R.A.; Austin, D.J.; Tolson, J.M.; VanMeter, S.A.; Lewis, E.W.; Derosier, F.J.; Lopez, M.C.; Kavanagh, S.T.; Miller, A.E.; et al. Subcutaneous ofatumumab in patients with relapsing-remitting multiple sclerosis: The MIRROR study. *Neurology* **2018**, *90*, e1805–e1814. [[CrossRef](#)]
100. Hauser, S.L.; Bar-Or, A.; Comi, G.; Giovannoni, G.; Hartung, H.-P.; Hemmer, B.; Lublin, F.; Montalban, X.; Rammohan, K.W.; Selmaj, K.; et al. Ocrelizumab versus Interferon Beta-1a in Relapsing Multiple Sclerosis. *N. Engl. J. Med.* **2017**, *376*, 221–234. [[CrossRef](#)]
101. James, M.L.; Hoehne, A.; Mayer, A.T.; Lechtenberg, K.; Moreno, M.; Gowrishankar, G.; Ilovich, O.; Natarajan, A.; Johnson, E.M.; Nguyen, J.; et al. Imaging B Cells in a Mouse Model of Multiple Sclerosis Using (64)Cu-Rituximab PET. *J. Nucl. Med.* **2017**, *58*, 1845–1851. [[CrossRef](#)] [[PubMed](#)]
102. Migotto, M.-A.; Mardon, K.; Orian, J.; Weckbecker, G.; Kneuer, R.; Bhalla, R.; Reutens, D.C. Efficient Distribution of a Novel Zirconium-89 Labeled Anti-cd20 Antibody Following Subcutaneous and Intravenous Administration in Control and Experimental Autoimmune Encephalomyelitis-Variant Mice. *Front. Immunol.* **2019**, *10*, 2437. [[CrossRef](#)] [[PubMed](#)]
103. Werner, J.M.; Lohmann, P.; Fink, G.R.; Langen, K.J.; Galldiks, N. Current Landscape and Emerging Fields of PET Imaging in Patients with Brain Tumors. *Molecules* **2020**, *25*, 1471. [[CrossRef](#)]
104. Dupont, A.C.; Largeau, B.; Guilloteau, D.; Santiago Ribeiro, M.J.; Arlicot, N. The Place of PET to Assess New Therapeutic Effectiveness in Neurodegenerative Diseases. *Contrast Media Mol. Imaging* **2018**, *2018*, 7043578. [[CrossRef](#)] [[PubMed](#)]
105. Werry, E.L.; Bright, F.M.; Pigué, O.; Ittner, L.M.; Halliday, G.M.; Hodges, J.R.; Kiernan, M.C.; Loy, C.T.; Kril, J.J.; Kassiou, M. Recent Developments in TSPO PET Imaging as A Biomarker of Neuroinflammation in Neurodegenerative Disorders. *Int. J. Mol. Sci.* **2019**, *20*, 3161. [[CrossRef](#)] [[PubMed](#)]
106. Beaino, W.; Janssen, B.; Vugts, D.J.; de Vries, H.E.; Windhorst, A.D. Towards PET imaging of the dynamic phenotypes of microglia. *Clin. Exp. Immunol.* **2021**, *206*, 282–300. [[CrossRef](#)]
107. Narayanaswami, V.; Dahl, K.; Bernard-Gauthier, V.; Josephson, L.; Cumming, P.; Vasdev, N. Emerging PET Radiotracers and Targets for Imaging of Neuroinflammation in Neurodegenerative Diseases: Outlook Beyond TSPO. *Mol. Imaging* **2018**, *17*, 1536012118792317. [[CrossRef](#)]
108. Zhang, L.; Hu, K.; Shao, T.; Hou, L.; Zhang, S.; Ye, W.; Josephson, L.; Meyer, J.H.; Zhang, M.-R.; Vasdev, N.; et al. Recent developments on PET radiotracers for TSPO and their applications in neuroimaging. *Acta Pharm. Sin. B.* **2021**, *11*, 373–393. [[CrossRef](#)]
109. Tiepolt, S.; Meyer, P.M.; Patt, M.; Deuther-Conrad, W.; Hesse, S.; Barthel, H.; Sabri, O. PET Imaging of Cholinergic Neurotransmission in Neurodegenerative Disorders. *J. Nucl. Med.* **2022**, *63*, 33s–44s. [[CrossRef](#)]
110. Ozenil, M.; Aronow, J.; Millard, M.; Langer, T.; Wadsak, W.; Hacker, M.; Pichler, V. Update on PET Tracer Development for Muscarinic Acetylcholine Receptors. *Pharmaceuticals* **2021**, *14*, 530. [[CrossRef](#)]
111. Tolosa, E.; Garrido, A.; Scholz, S.W.; Poewe, W. Challenges in the diagnosis of Parkinson's disease. *Lancet Neurol.* **2021**, *20*, 385–397. [[CrossRef](#)] [[PubMed](#)]
112. Waszkiewicz, N. Mentally Sick or Not-(Bio)Markers of Psychiatric Disorders Needed. *J. Clin. Med.* **2020**, *9*, 2375. [[CrossRef](#)] [[PubMed](#)]
113. Taylor, S.F.; Tso, I.F. GABA abnormalities in schizophrenia: A methodological review of in vivo studies. *Schizophr. Res.* **2015**, *167*, 84–90. [[CrossRef](#)] [[PubMed](#)]
114. Parot, V.; Herraiz, J.L.; Dave, S.R.; Udías, J.M.; Moore, S.C.; Park, M.-A.; Vaquero, J.J.; Lage, E. *A New Approach for Multiplexed PET Imaging*; IEEE NSS-MIC: Seoul, Korea, 2013.
115. Slart, R.H.J.A.; Tsoumpas, C.; Glaudemans, A.W.J.M.; Noordzij, W.; Willemsen, A.T.M.; Borra, R.J.H.; Dierckx, R.A.J.O.; Lammermsma, A.A. Long axial field of view PET scanners: A road map to implementation and new possibilities. *Eur. J. Nucl. Med. Mol. Imaging* **2021**, *48*, 4236–4245. [[CrossRef](#)]

116. Surti, S.; Pantel, A.R.; Karp, J.S. Total Body PET: Why, How, What for? *IEEE Trans. Radiat. Plasma Med. Sci.* **2020**, *4*, 283–292. [[CrossRef](#)] [[PubMed](#)]
117. Miller-Thomas, M.M.; Benzinger, T.L. Neurologic Applications of PET/MR Imaging. *Magn. Reson. Imaging Clin. N. Am.* **2017**, *25*, 297–313. [[CrossRef](#)]

Disclaimer/Publisher’s Note: The statements, opinions and data contained in all publications are solely those of the individual author(s) and contributor(s) and not of MDPI and/or the editor(s). MDPI and/or the editor(s) disclaim responsibility for any injury to people or property resulting from any ideas, methods, instructions or products referred to in the content.